

---

# Crystal structure of Ski8p, a WD-repeat protein with dual roles in mRNA metabolism and meiotic recombination

---

ZHIHONG CHENG,<sup>1</sup> YUYING LIU,<sup>1</sup> CHERNHOE WANG,<sup>1</sup> ROY PARKER,<sup>2</sup> AND HAIWEI SONG<sup>1,3</sup>

<sup>1</sup>Laboratory of Macromolecular Structure, Institute of Molecular and Cell Biology, Singapore 117609

<sup>2</sup>Department of Molecular and Cellular Biology and Howard Hughes Medical Institute, University of Arizona, Tucson, Arizona 85721, USA

<sup>3</sup>Department of Biological Sciences, National University of Singapore, Singapore 117543

(RECEIVED May 10, 2004; FINAL REVISION June 14, 2004; ACCEPTED June 20, 2004)

## Abstract

Ski8p is a WD-repeat protein with an essential role for the Ski complex assembly in an exosome-dependent 3'-to-5' mRNA decay. In addition, Ski8p is involved in meiotic recombination by interacting with Spo11p protein. We have determined the crystal structure of Ski8p from *Saccharomyces cerevisiae* at 2.2 Å resolution. The structure reveals that Ski8p folds into a seven-bladed β propeller. Mapping sequence conservation and hydrophobicities of amino acids on the molecular surface of Ski8p reveals a prominent site on the top surface of the β propeller, which is most likely involved in mediating interactions of Ski8p with Ski3p and Spo11p. Mutagenesis combined with yeast two-hybrid and GST pull-down assays identified the top surface of the β propeller as being required for Ski8p binding to Ski3p and Spo11p. The functional implications for Ski8p function in both mRNA decay and meiotic recombination are discussed.

**Keywords:** mRNA decay; meiotic recombination; protein crystallography; WD-repeat

mRNA turnover is important in eukaryotic cells and functions in modulating gene expression, antiviral defense, and mRNA surveillance, wherein aberrant mRNAs are recognized and degraded (Frischmeyer and Dietz 1999; van Hoof and Parker 1999; Waterhouse et al. 2001; Parker and Song 2004). Two major pathways of general mRNA decay have been characterized in both yeast and mammals (Tucker and Parker 2000; Mitchell and Tollervey 2001). In both pathways, mRNA decay initiates with the shortening of the 3'-poly(A) tail of mRNAs by a variety of nucleases (for review, see Parker and Song 2004). Following deadenylation, the 5' cap structure can be removed by the Dcp1p/Dcp2p complex, allowing exonucleolytic decay by Xrn1p. Alter-

natively, the deadenylated mRNAs can be degraded 3' to 5' by the cytoplasmic exosome, which is a highly conserved 10 subunit complex of 3'-to-5' exonucleases (Mitchell et al. 1997; Jacobs Anderson and Parker 1998; Allmang et al. 1999; Chen et al. 2001; Wang and Kiledjian 2001; Mukherjee et al. 2002).

The exosome also functions in two specialized mRNA decay pathways that recognize and degrade aberrant mRNAs. For example, in a process referred to as nonsense-mediated mRNA decay (NMD), transcripts with premature translation termination codons are degraded either by deadenylation-independent decapping (5'-to-3' NMD), or by accelerated deadenylation and 3'-5' exonucleolytic digestion by the exosome (3'-to-5' NMD; Muhrad and Parker 1994; Cao and Parker 2003; Lejeune et al. 2003; Mitchell and Tollervey 2003; Takahashi et al. 2003). In addition, in a process referred to as nonstop decay (NSD), mRNAs lacking translation termination codons are recognized and rapidly degraded 3' to 5' by the cytoplasmic exosome (Frischmeyer et al. 2002; Maquat 2002; van Hoof et al. 2002). Thus, in all

---

Reprint requests to: Haiwei Song, Laboratory of Macromolecular Structure, Institute of Molecular and Cell Biology, 30 Medical Drive, Singapore 117609; e-mail: haiwei@imcb.a-star.edu.sg; fax: (0)65 68727007.

Article published online ahead of print. Article and publication date are at <http://www.proteinscience.org/cgi/doi/10.1110/ps.04856504>.

the 3'-to-5' mRNA decay pathways characterized so far, degradation of the deadenylated mRNA involves the exosome.

The function of the exosome in cytoplasmic mRNA turnover requires several cofactors including the putative GTPase Ski7p, and the Ski complex consisting of Ski2p, Ski3p, and Ski8p (Araki et al. 2001; Maquat 2002; Takahashi et al. 2003). These superkiller (*SKI*) genes were initially identified from mutations that cause overexpression of a killer toxin encoded by the endogenous double-stranded RNA (Toh et al. 1978). Subsequent work demonstrated that the products of *SKI2*, *SKI3*, and *SKI8* genes are necessary for the 3'-to-5' mRNA degradation and repression of translation of nonpolyadenylated RNA in addition to their antiviral activities (Masison et al. 1995; Jacobs Anderson and Parker 1998; Araki et al. 2001). Ski2p and Ski3p are a putative RNA helicase and a tetratricopeptide repeat (TPR) protein, respectively, while Ski8p is a WD-repeat containing protein (Rhee et al. 1989; Matsumoto et al. 1993; Widner and Wickner 1993). The three Ski proteins form a stable complex with 1:1:1 stoichiometry, and the complex is localized in the cytoplasm (Brown et al. 2000). The Ski complex has been suggested to be an mRNA decay-specific cofactor for the exosome because mutations in the *SKI* genes inhibit 3'-to-5' mRNA decay, but have no effect on functions of exosome in nuclear RNA processing (Jacobs Anderson and Parker 1998; Brown et al. 2000; van Hoof et al. 2000). However, the nature of physical interactions within the Ski complex and with the exosome, and the specific role of the Ski complex in 3' mRNA decay remain elusive. Recently, it has been shown that the different regions of the N-terminal domain of Ski7p interact with the exosome and the Ski complex, respectively, thereby recruiting both the Ski complex and the exosome to the 3' end of mRNA for degradation (Araki et al. 2001).

Within the Ski complex, the Ski8p is particularly interesting. In addition to Ski8p function in mRNA decay, yeast strains lacking Ski8p have strong reductions in meiotic recombination, but have no detectable effects on mitotic recombination or DNA repair (Malone et al. 1991; Evans et al. 1997; Gardiner et al. 1997; Fox and Smith 1998; Pecina et al. 2002). Moreover, this meiotic role of Ski8 appears to be conserved (Evans et al. 1997; Fox and Smith 1998; Tesse et al. 2003; Arora et al. 2004). However, because of its direct role in mRNA decay, the meiotic role of Ski8 has been unclear, and could have been an indirect effect of defects in 3'-to-5' mRNA decay.

Several observations now argue that Ski8p has a distinct role in meiosis separate from its function in mRNA decay. First, although *ski8Δ* yeast strains show defects in meiosis, *ski2Δ* or *ski3Δ* strains, which equally affect mRNA decay, do not affect meiotic recombination (Arora et al. 2004). Second, and more direct, Ski8p shows strong physical interactions with Spo11p, which is homologous to the ar-

chaeal topoisomerases. Spo11p acts in concert with at least nine other proteins (including Ski8p) to create DNA double-strand breaks (DSBs), whose repair leads to meiotic recombination (Tesse et al. 2003; Arora et al. 2004). Third, the Ski8 mRNA is induced ~15 times on entry to meiosis (Gardiner et al. 1997), and the Ski8 protein redistributes from the cytoplasm to the nucleus and localizes to chromosomes specifically during meiosis (Arora et al. 2004). These results indicate that Ski8p plays distinct roles in meiotic recombination and mRNA decay by changing its localization and interacting with the different protein partners by as yet undetermined interactions.

Possible insight into how Ski8p interacts with other proteins comes from analysis of the Ski8p sequence. Ski8p contains multiple repeats of the "WD" motif, originally identified in  $\beta$ -transducin (Matsumoto et al. 1993; Evans et al. 1997). These motifs are found in many proteins with diverse functions, and are thought to mediate protein-protein interactions (Smith et al. 1999). To date, several crystal structures of WD-repeat proteins have been solved including the G protein  $\beta$ -subunit (Wall et al. 1995; Gaudet et al. 1996; Lambright et al. 1996; Sondek et al. 1996), the C-terminal  $\beta$  propeller domain of Tup1 (Tup1c), and its human homolog Groucho/TLE1 protein (hTle1-C; Sprague et al. 2000; Pickles et al. 2002;), the Aip1p protein involved in actin depolymerization (Voegtli et al. 2003), and the F-box protein  $\beta$ -TrCP1 in complex with Skp1 and the  $\beta$ -catenin peptide (Wu et al. 2003). A common feature of these structures is the arrangement of the "WD" motifs in a bladed  $\beta$  propeller, thereby presenting possible protein interactions surfaces on the top, bottom, and side of the propeller structure.

To gain insight into the functional roles Ski8 plays in the 3'-to-5' mRNA decay and DSB formation in meiotic recombination, we determined the crystal structure of the full-length Ski8p protein from *Saccharomyces cerevisiae*. As expected, the protein folds into a seven-bladed  $\beta$  propeller similar to other "WD" motif containing proteins. Mapping the sequence conservation and hydrophobicity on the molecular surface of Ski8p revealed a conserved hydrophobic patch located on the top face of the  $\beta$  propeller. Mutagenesis combined with yeast two-hybrid and GST pull-down assays suggest that this site is involved in interactions with Ski3p and Spo11p. The structure provided a starting point for further studies on the Ski complex assembly and the molecular basis of Ski complex mediated 3' to 5' mRNA decay, as well as the functional role of Ski8p in meiotic recombination.

## Results

### Structure determination

The full-length Ski8p from *S. cerevisiae* was expressed in *Escherichia coli* and purified to homogeneity. Orthorhom-

bic crystals were obtained by macroseeding method, containing one molecule per asymmetric unit (AU). For phasing, multiwavelength anomalous dispersion (MAD) data were measured from a seleno-methionine derivative that yielded an easily interpretable electron density map at 2.2 Å resolution, allowing 80% of the model to be built automatically. The current model has been refined to a resolution of 2.2 Å with working and free *R* factors of 24.6% and 27.9%, respectively. Five regions of the polypeptide chain are not visible in the electron density map, and are assumed to be disordered, namely, residues 101–104, residues 133–136, residues 225–233, residues 277–287, and residues 370–375. Statistics of structure determination and refinement are summarized in Table 1 (see Materials and Methods).

### Overall structure description

As shown in Figure 1, the polypeptide chain of Ski8p folds into a seven-bladed β propeller similar to that observed in the β-subunits of heterotrimeric G proteins (Gβ) and in the C terminus of the yeast transcriptional repressor Tup1 (Tup1c). The propeller fold is characterized by seven blades that are pseudosymmetrically arranged around a central axis. Each blade consists of a four-stranded antiparallel β

sheet, with the strands in each blade (labeled A–D) running approximately parallel to the pseudoseven-fold axis, and ranging from the inside to the outside of the propeller. The center of the propeller is formed by the edges of the seven “A” strands, which delineate an axial channel running through the center of the propeller, which is filled with a large number of very well-ordered solvent molecules. The eponymous Trp–Asp motif is only present in blades 1 and 6 in Ski8p (Fig. 2), being replaced by other amino acids in blades 2, 3, 4, 5, and 7. Blades 1–6 are formed by contiguous segments of the polypeptide chain. In blade 7, the innermost three strands come from the extreme C terminus while the outmost strand is provided by a strand from N terminus.

### Comparison with other WD repeat proteins

Although the sequence of Ski8p shows only 15.5% of identity with Gβ and 18.5% of identity with Tup1c, the β propeller of Ski8p superimposes strikingly well with Gβ with an RMSD of 1.5 Å over 238 Cα atoms, and with Tup1c, with an RMSD of 1.3 Å over 233 Cα atoms (Fig. 3A,B). The structure of a single blade is strikingly conserved both within the Ski8p structure (Fig. 3C), and between Ski8p

**Table 1.** Data collection, phase determination, and refinement statistics

	Se-Met MAD data		
	λ1 (peak)	λ2 (edge)	λ3 (remote)
Wavelength (Å)	0.9789	0.9791	0.9724
Resolution (Å)	2.2	2.3	2.3
Unique reflections (N)	21,256	21,243	21,599
Completeness (%)	98.8 (100)	98.9 (99.9)	99.8 (99.9)
Redundancy	3.5	3.5	3.5
<i>I</i> / <i>σ</i> ( <i>I</i> )	10.3 (2.0)	8.7 (2.1)	7.5 (2.0)
<i>R</i> <sub>merge</sub> (%) <sup>a</sup>	6.3	7.3	8.6
Number of sites	4		
Figure of merit			
Before density modification		0.37	
After density modification		0.59	
Refinement statistics			
Resolution range (Å)		2.2	
Reflection used		17,717	
<i>R</i> <sub>cryst</sub> <sup>b</sup>		24.6	
<i>R</i> <sub>free</sub> <sup>c</sup>		27.9	
Nonhydrogen atoms			
Protein (N)		2816	
Waters (N)		159	
r.m.s. deviations			
Bond length (Å)		0.007	
Bond angle (°)		1.06	

Values in parentheses indicate the specific values in the highest resolution shell.

<sup>a</sup>  $R_{\text{merge}} = \sum |I_j - \langle I \rangle| / \sum I_j$ , where  $I_j$  is the intensity of an individual reflection, and  $\langle I \rangle$  is the average intensity of that reflection.

<sup>b</sup>  $R_{\text{cryst}} = \sum ||F_o| - |F_c|| / \sum |F_o|$ , where  $F_o$  denotes the observed structure factor amplitude, and  $F_c$  denotes the structure factor amplitude calculated from the model.

<sup>c</sup>  $R_{\text{free}}$  is as for  $R_{\text{cryst}}$  but calculated with 5.2% of randomly chosen reflections omitted from the refinement.

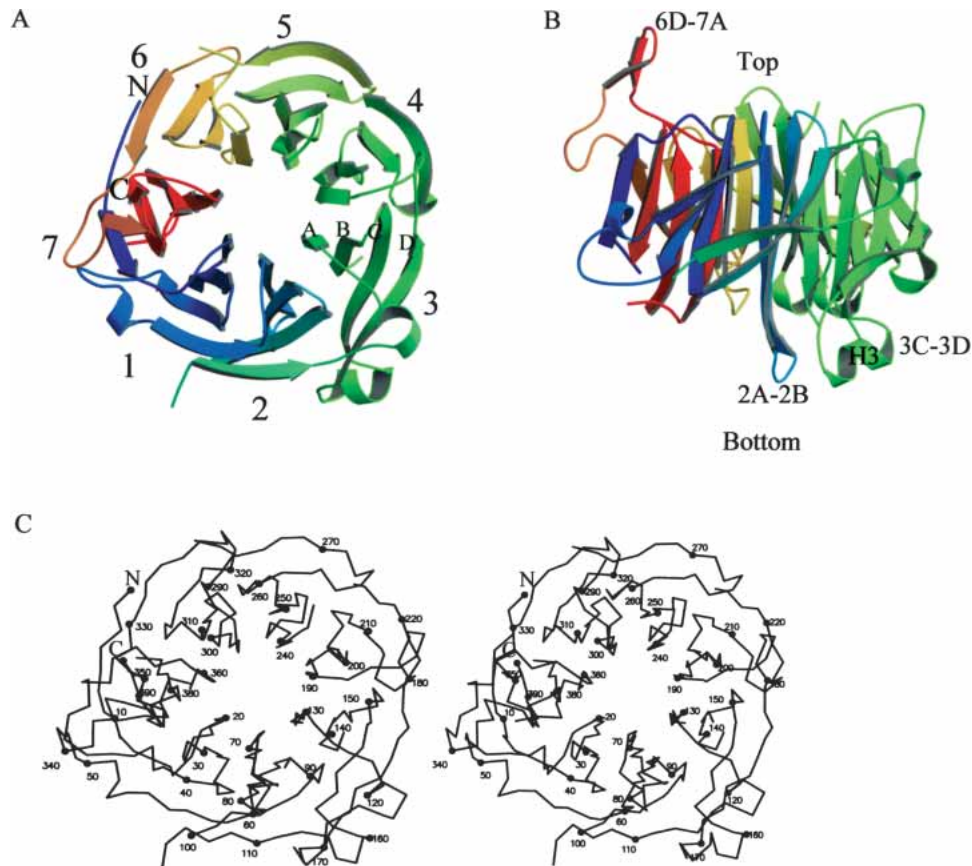


**Figure 1.** Overall structure of Ski8p. (A) Ribbon diagram of Ski8p showing the seven-bladed  $\beta$  propeller structure. Each blade consists of a four-stranded  $\beta$ -sheet (labeled A–D). The view is looking down the central axis of the propeller onto the “top” surface. The top surface is defined by the presence of the D–A loops connecting sequential blades. (B) View rotated  $90^\circ$  about the horizontal axis in A, looking at the propeller from the side. The top face and bottom face are marked according to the convention for WD-repeat protein structure. (C) Stereo view of a C $\alpha$  trace of Ski8p with every tenth residue labeled and marked with a closed circle. Figures 1, 3, 4C, and 5 were generated using MOLSCRIPT (Kraulis 1991).

blades and individual blades in G $\beta$  and Tup1c. For instance, blade 1 of Ski8p superimposes with other Ski8p blades with C $\alpha$ –C $\alpha$  RMSD of 0.9–1.4 Å, and with a typical blade of G $\beta$ , blade 4 or with a typical blade of Tup1c, blade 3, with the same RMSD of 1.2 Å. The “structural tetrad” or hydrogen-bonding network, as described in G $\beta$  and Tup1c (Wall et al. 1995; Lambright et al. 1996; Sprague et al. 2000), is also observed, but only in blades 1 and 6 of Ski8p propeller (Fig. 3D). This tetrad is formed between Trp in strand C, Ser/Thr in strand B, His in the DA loop, and the nearly invariant Asp in the tight turn between strands B and C.

Despite the similarities, some structural differences exist between the propeller of Ski8p and those of G $\beta$  and Tup1c. The most notable differences occur in N terminus and the loop regions. Ski8p lacks the N-terminal extension G $\beta$  and Tup1c have. In G $\beta$ , the N-terminal extension forms an  $\alpha$ -helix, which participates in a coil–coil with the N-terminal segment of the G $\gamma$  subunit in the trimeric G protein

complex (Wall et al. 1995; Lambright et al. 1996). The N-terminal 50 amino acids in Tup1c forms a subdomain that is joined to the propeller by  $\beta$ -sheet interactions that extend blade 6 into a six-stranded sheet (Fig. 3A), while the similar region in hTle1-C forms a  $\beta$ -hairpin that extends blade 5 into a six-stranded sheet (Sprague et al. 2000; Pickles et al. 2002). In Ski8p, the 6D–7A loop, which is ~26 residues long, protrudes from the top face of the propeller (Figs. 1B, 3B). Because this loop is only present in Ski8p and not in other Ski8p homologs (Fig. 2), it is not likely to be central to Ski8p function, and is probably involved in yeast-specific functions. Loop 2A–2B connects strands 2A and 2B, which are substantially longer than their corresponding strands in both G $\beta$  and Tup1c (Fig. 3B). The 3C–3D loop stretches out from the bottom face, and contains a short helix. Such loop structure is not observed in both G $\beta$  and Tup1c (Fig. 3B), but is conserved in Ski8 across species (Fig. 2). Interestingly, strand 3D seems only present in Ski8 from *S. cerevisiae* (ScSki8) and *Sordaria macrospora* (SmSki8) but not in

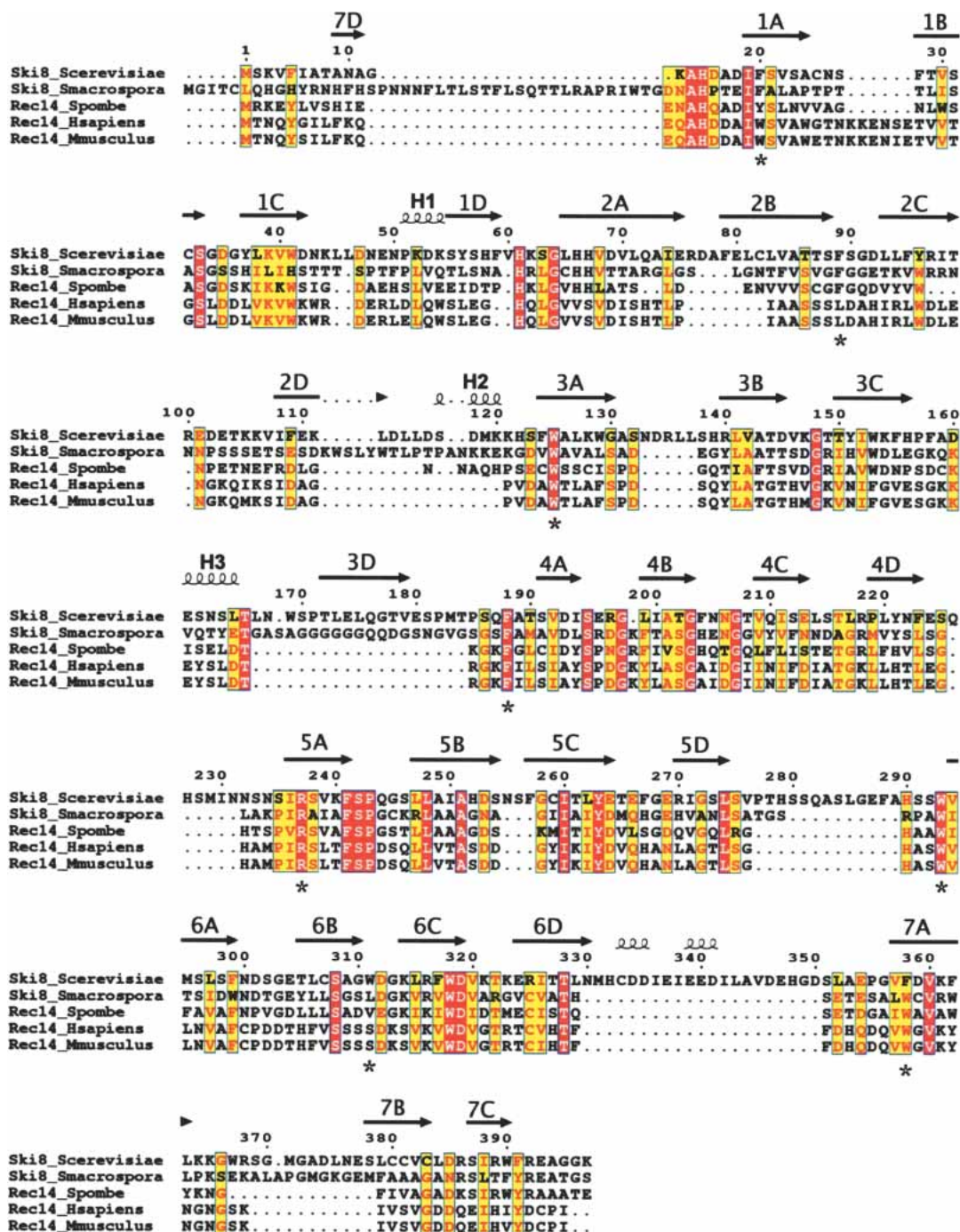
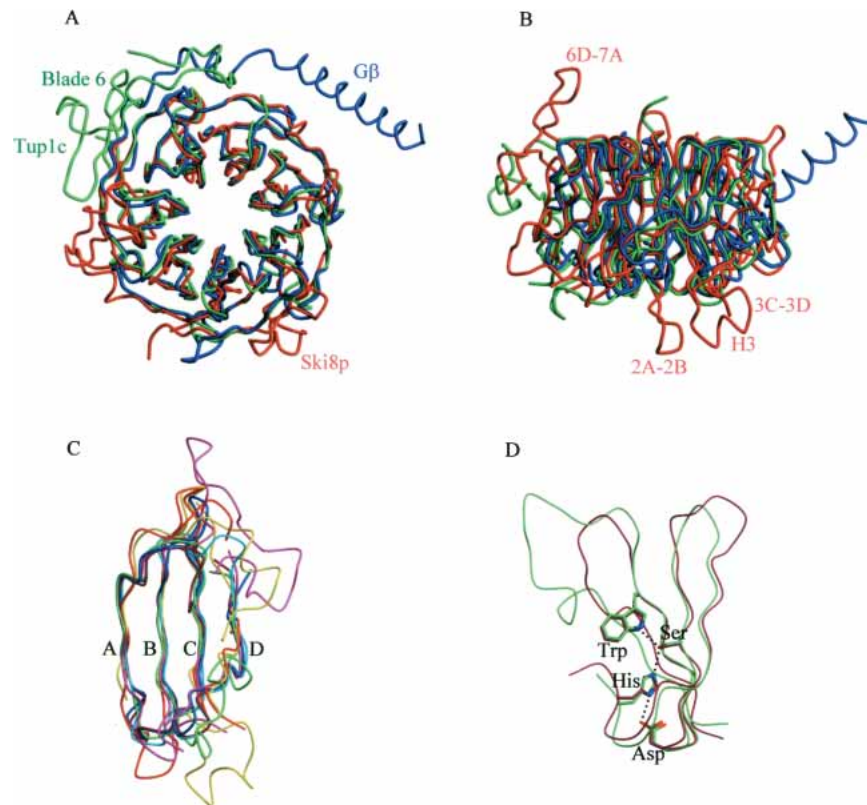


Figure 2. Sequence alignment of *S. cerevisiae* Ski8, *S. macrospora* Ski8, *Schizosaccharomyces pombe* Rec14, *Homo sapiens* Rec14, and *Mus musculus* Rec14. The secondary structures of *S. cerevisiae* Ski8 are shown. Invariant residues are white letters, similar residues are red, and others are black. Residues speculated for interactions with Ski3 and Spo11 are indicated by \*.

the rest of the Ski8 homologs (Fig. 2). Because strand 3D is essential for formation of blade 3 and structurally conserved in Ski8p, G $\beta$ , and Tup1c, it is likely that Ski8 homologs other than ScSki8 and SmSki8 may use part of the 3C–3D loop to form strand 3D.

#### Location of protein–protein interaction sites on the $\beta$ propeller

Previous analyses indicated that Ski8p interacts with Ski3p and/or Ski2p in 3'-to-5' mRNA decay, and Spo11p during



**Figure 3.** Comparison of Ski8p with G $\beta$  and Tup1c. (A) Superposition of Ski8p, G $\beta$ , and Tup1c. Ski8p is shown in red, G $\beta$  in blue, and Tup1c in green. The view of Ski8p is as in Figure 1A. (B) Same as A but with the view looking at the side of the propeller. (C) Superposition of all seven blades of Ski8p. The C $\alpha$  backbone for each of the seven blades was aligned with respect to blade 1. Four strands of each blade are indicated by A, B, C, and D. Blade 1, green; blade 2, red; blade 3, yellow; blade 4, cyan; blade 5, blue; blade 6, maroon; blade 7, magenta. (D) Superposition of two typical blades, blade 1 (green) and blade 6 (maroon) containing the eponymous Trp–Asp motif. Four conserved residues, which are involved in the structural tetrad, are shown in stick models, and hydrogen bonds are indicated with dashed lines.

meiotic recombination (Brown et al. 2000; Arora et al. 2004). To identify the key regions on the surface of Ski8p, which are likely to be involved in interaction with Ski3p, Ski2p, and Spo11p, we mapped the sequence conservation shared by eukaryotic Ski8p proteins on the molecular surface of the budding yeast Ski8p structure. This analysis revealed a prominent conserved patch that is situated on the top face of the  $\beta$  propeller and encompasses nearly all of the DA and BC loops (Fig. 4A). Moreover, mapping of the side chains of hydrophobic residues on the molecular surface of Ski8p reveals that a large hydrophobic patch consisting of residues F20, F89, W125, F188, W293, W311, and F358 is located on the top face of the  $\beta$  propeller, overlapping with the conserved patch identified by conservation mapping (Fig. 4B,C). The presence of such a conserved patch of hydrophobic residues suggests this region is a site of protein–protein interaction. Inspection of both the side and bottom surfaces of the propeller shows that there is no obvious conserved or hydrophobic patch, which is large enough for potential protein–protein interactions (data not shown).

Consistent with the top face of Ski8p being a site of protein interaction, we note that in the Ski8p crystal lattice, loops 3C–3D and 2A–2B from symmetry-related molecules bind to the top surface area, burying a pairwise accessible surface area of 1260 Å<sup>2</sup>. The interactions of loops 3C–3D and 2A–2B with the top face are predominantly hydrophobic in nature with some additional hydrogen bonds. The top surface that interacts with loops 3C–3D and 2A–2B is composed mainly of hydrophobic amino acids (F20, F89, V146, K147, F188, N205, R237, W293, M295, W311, and F358; Fig. 5A). Among them, F20, F188, R237, W293, M295, and F358 are located in the DA loop of blades 1, 4, 5, 6, and 7, respectively, and F89, V146, K147, N205, and W311 lie in the BC loop of blades 2, 3, 4, and 6, respectively. Most of these residues are highly conserved in Ski8 homologs across species, except for V146, N205, and W311 (Fig. 2). The surface area of loops 3C–3D and 2A–2B that interacts with the top face consists of hydrophobic residues A78, L165, L167, and the additional polar and charged residues R76, D77, D160, E161, S162, and T166 (Fig. 5A). Among them,

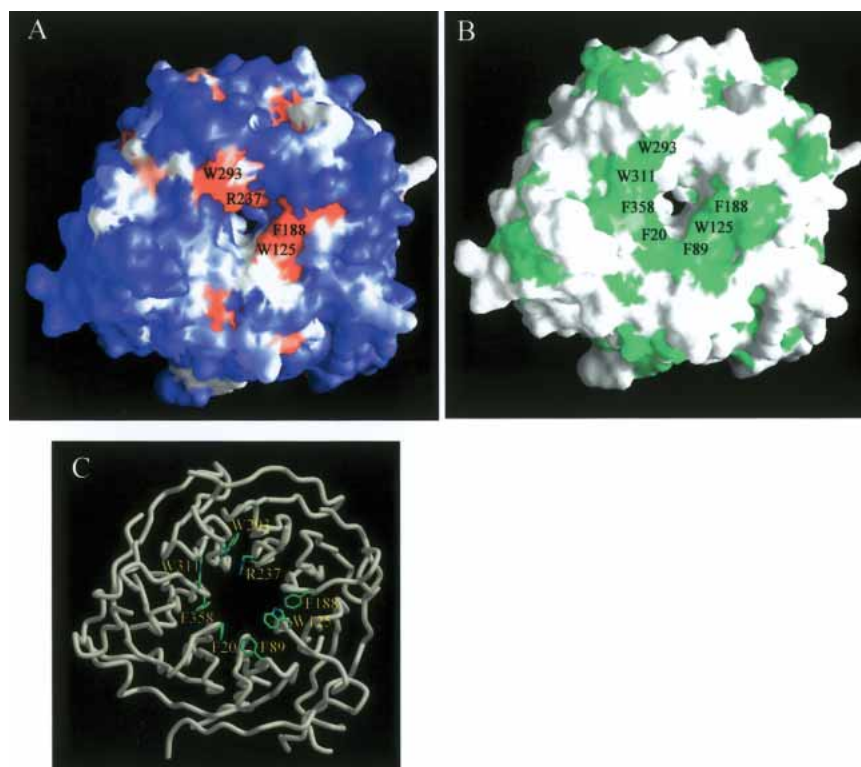


**Figure 4.** Molecular surface views of Ski8p. (A) Surface representation of Ski8p showing the regions of high-to-low sequence conservation shared by the eukaryotic Ski8 proteins, corresponding to a color ramp from red to blue, respectively. Invariant residues are labeled. The view is as in Figure 1A. (B) Molecular surface of Ski8p colored according to residue property, with hydrophobic residues green and other residues gray. The hydrophobic residues are labeled. The view is as in A. (C) The worm model showing the C $\alpha$  backbones of Ski8p. Residues located either in hydrophobic patch or in conserved patch are shown in stick models. The view is as in A. A and B were produced using GRASP (Nicholls et al. 1991).

only E161 and T166 are highly conserved across species (Fig. 2). These results suggest that the top face of the  $\beta$  propeller of Ski8p is a hydrophobic patch, and is likely involved in binding Ski3p, Ski2p, and Spo11p or other unidentified interacting proteins.

#### Mutational analysis of Ski8p

Evidence suggests that Ski8p interacts directly with the Ski3p and Spo11p proteins, and may interact directly, or in combination with Ski3p to Ski2p. Specifically, coimmunoprecipitation showed that Ski3p interacts with Ski8p without the involvement of Ski2p (Brown et al. 2000). However, Ski2p did not associate with Ski3p in the absence of Ski8p, nor did Ski2p associate with Ski8p in the absence of Ski3p, suggesting that the binary complex formed by Ski3p and Ski8p is required for stable binding of Ski2p to Ski8p and/or Ski3p. Moreover, Ski8p also interacts directly with Spo11p, and participates in meiotic recombination (Arora et al. 2004). However, the structural mechanism of these interactions has not been elucidated, and the amino acid residues

critical for Ski8p interaction with Ski3p, Spo11p, or possibly Ski2p, have not been identified.

Conservation and hydrophobicity mapping suggested that the top face of the  $\beta$  propeller of Ski8p is likely involved in the interaction of Ski8p with its binding partners. To examine the role of the amino acids located on the top face of Ski8p play in mediating interactions with Ski3p, Ski2p, and Spo11p, a Ski8p variant where the top surface was altered was created by site-directed mutagenesis. The resulting variant Ski8p protein was examined for its ability to bind to Ski3p, Ski2p, and Spo11p by yeast two-hybrid and GST pull-down assays. In the latter assay, wild-type and mutant Ski8p were immobilized on glutathione-Sepharose and examined for their binding to Ski3p and Spo11p translated *in vitro* in the presence of  $^{35}\text{S}$ -methionine. The specific mutant created (referred to as “top” mutant) contains alanine substitutions of six residues (F20A, F89A, W125A, W293A, W311A, and F358A) located at the hydrophobic patch plus R237, a well-conserved residue in the Ski8 family found with the conserved top surface. An important result was the alteration of the top surface of Ski8p substantially reduced binding of Ski8p to either Ski3p or Spo11p (Fig. 6A,B).

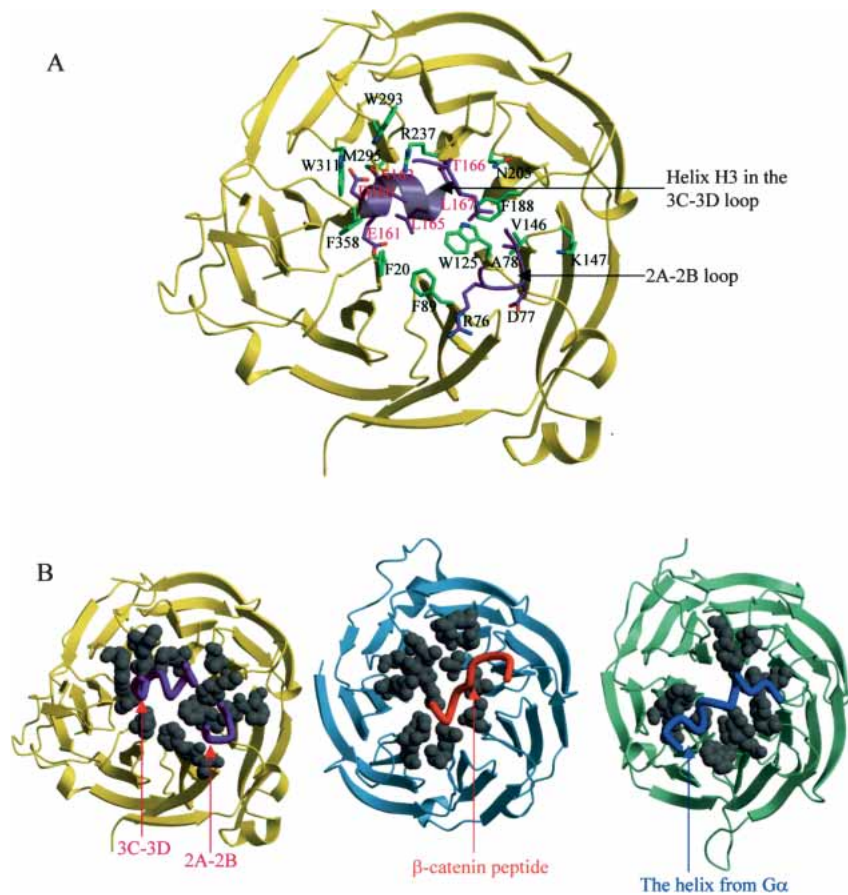


**Figure 5.** Location of the protein–protein interactions site on the top face of the  $\beta$  propeller. (A) Close-up view of the interface between the top face of the  $\beta$  propeller in Ski8p (yellow) and the loops of 2A–2B and 3C–3D from the symmetry related molecule (purple). Residues involved in the interface are shown in stick models. (B) Comparison of the protein–protein interactions on the top surface for three WD-repeat proteins. (Left) The top face of Ski8p (yellow) interacting with its symmetry related loop regions 3C–3D and 2A–2B (purple). (Middle) The top face of  $\beta$ -TrCP1 WD-40 domain (sky blue) with bound doubly phosphorylated  $\beta$ -catenin peptide (red). pdb code: 1p22. (Right) The top face of  $G\beta$  (light green) interacting with the helix of  $G\alpha$  (blue). pdb code: 1gp2. All residues involved in interaction on the top face of the  $\beta$  propeller are shown in CPK model.

These results indicate that the top surface of Ski8p is required for binding to Ski3p and Spo11p, although the possibility of whether there are additional contacts between Ski3p and Spo11p to the side surface of Ski8p cannot be excluded (see below).

Interestingly, mutation of the Ski8p top surface appears to have little effect on the binding of Ski8p to Ski2p (Fig. 6C). This suggests that interactions between Ski2p and Ski8p do not require the top surface, and therefore, a Ski8p–Ski2p interaction is likely to involve a different surface of the Ski8p. In addition, because the “top” mutant strongly inhibits Ski8p–Ski3p interaction, this result raises the possibility that Ski8p and Ski2p directly interact even in the absence of Ski3p. The fact that the “top” mutant still interacts with Ski2p implies that these mutations present in the Ski8p “top” mutant have not grossly altered the overall structure of the Ski8p, consistent with the changes simply being changes in surface structure. Finally, our results sug-

gest that the binding of Spo11p to Ski8p may also involve interactions with the side of the  $\beta$  propeller structure. Specifically, mutation of residue F59 located at the side surface to alanine (F59A) caused a substantial reduction of binding to Spo11p, but did not affect the binding of Ski8p to Ski3p (Fig. 6A,B).

## Discussion

Solving the structure of Ski8p has revealed that this protein folds into a classic  $\beta$  propeller structure similar to the known structures of other WD motif-containing proteins. In addition, the Ski8p structure and experimental analysis presents evidence that the top surface of the Ski8p  $\beta$  propeller structure functions as a site of protein–protein interactions, and is required for interactions between Ski8p and both Ski3p and Spo11p. This conclusion is based on the

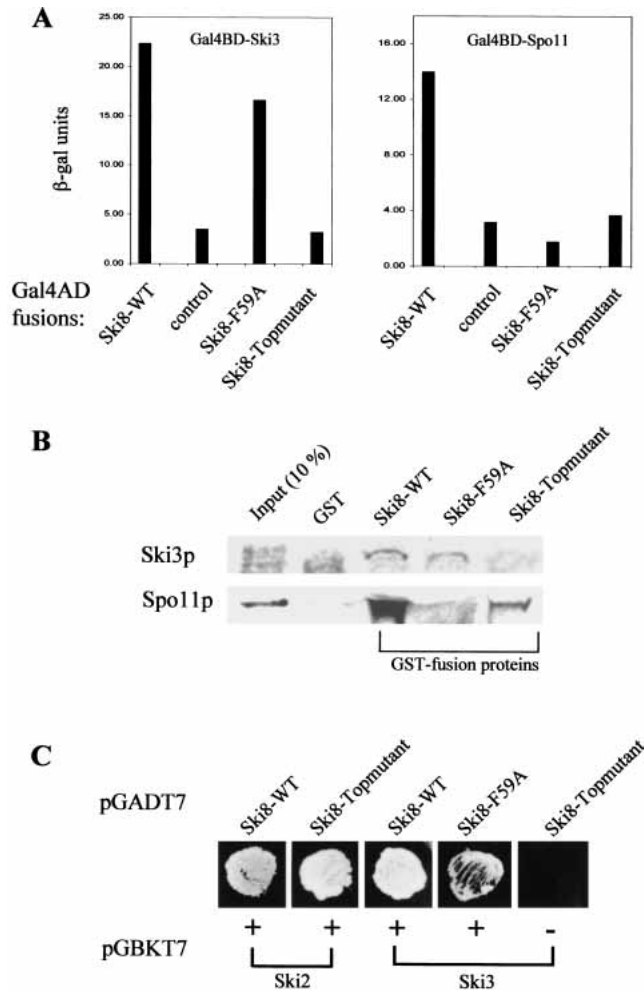


**Figure 6.** Mutational analysis of Ski8p mutants. (A) Effects of mutations at the top surface of the  $\beta$  propeller on the interactions of Ski8p with Ski3p and Spo11p, respectively.  $\beta$ -Galactosidase activity from various transformants estimated as described under Materials and Methods. The Ski8p-topmutant refers to a mutant Ski8p protein where seven residues (F20A, F89A, W125A, R237A, W293A, W311A, and F358A) were mutated to alanine. (Left) Ski8p versus Ski3p. (Right) Ski8p versus Spo11p. (B) Ski3p and Spo11p were translated *in vitro* in the presence of  $^{35}\text{S}$ -methionine and examined for binding to the immobilized Ski8p variants. (C) Effects of mutations at the top surface of the  $\beta$  propeller on the interactions of Ski8p with Ski2p, Ski3p, respectively. Alanine substitutions for seven top residues of Ski8p (Ski8p-topmutant) abolish the two-hybrid interaction between Ski3p and Ski8p, whereas such mutations have no effect on the interactions between Ski2p and Ski8p. Plus and minus signs indicate positive and negative interactions, respectively. F59A serves as negative control.

presence of a conserved patch of largely hydrophobic residues on the top surface (Fig. 4A), and on the observation that mutation of this surface disrupts two hybrid interactions between Ski8p and both Ski3p and Spo11p (Fig. 6).

Similar to Ski8p, several other WD-repeat proteins use their top faces for interacting with their protein partners. For example, in the structure of heterotrimeric G protein, the top face of G $\beta$  mediates its interaction with G $\alpha$ -GDP (Wall et

al. 1995; Lambright et al. 1996; Fig. 5B). Moreover, the structure of the  $\beta$ -TrCp1-Skp1- $\beta$ -catenin ternary complex shows that the  $\beta$ -catenin peptide binds the top face of the  $\beta$  propeller of  $\beta$ -TrCp1 (Wu et al. 2003; Fig. 5B). Similarly, the structure of G $\beta$  complexed with phosducin showed that the N-terminal domain of phosducin interacts with all of the top loops of the  $\beta$  propeller of G $\beta$  (Gaudet et al. 1996). Finally, 11-point mutations in the yeast Tup1p that specifically affect its interaction with Mat $\alpha$ , a promoter-specific DNA-binding protein, have been mapped on the top face of the Tup1c propeller (Komachi and Johnson 1997; Sprague et al. 2000). Taken together, these results suggest that the top face of the propeller is a site for protein-protein interactions that may be conserved in WD repeat domains in general, although the specific residues involved in protein-protein interaction in the individual WD repeat domains may vary.

These results suggest a model for the assembly of the Ski complex involved in mRNA decay wherein the Ski8p plays an important role in bringing Ski3p and Ski2p together. Because mutation of the top surface of Ski8p affects Ski3p binding, but does not appear to affect Ski8p-Ski2p interaction, we suggest that the complex involves the following interactions. First, interactions between the top surface of Ski8p and Ski3p would nucleate the complex, and based on the coimmunoprecipitation experiments and our GST pull-down assay are stable enough to persist even in the absence of Ski2p (Brown et al. 2000). Moreover, because TPR and WD-repeat proteins are often found in association with each other (Goebel and Yanagida 1991; van der Voorn and Ploegh 1992; Neer et al. 1994; Smith et al. 1999), a reasonable hypothesis is that the TPR domain of Ski3p interacts with Ski8p. Second, we suggest that Ski2p has interactions with either the side or bottom of Ski8p, which are stabilized by additional interactions between Ski2p and Ski3p. Although this model is supported by some experimental evidence, it should be considered speculative until more information is obtained. However, it should be noted that this model is different, and more consistent with the available evidence, than a predicted structure of the Ski complex based on computational methods (Aloy et al. 2004).

Ski8p is an interesting protein because it has been shown to be essential in two distinct cellular processes: mRNA metabolism and meiotic recombination. Moreover, emerging information shows that Ski8p plays fundamentally different roles in RNA metabolism and DSB formation during meiotic recombination. In 3'-to-5' mRNA decay, Ski8p localizes predominantly to the cytoplasm and interacts with Ski2p and Ski3p to form the Ski complex, thereby mediating the exosome-dependent mRNA decay. During meiotic recombination, Ski8p relocates from the cytoplasm to the nucleus and interacts with Spo11p, thus either affecting the ability of Spo11p to bind DNA or acting in concert with Spo11p to recruit Rec102p and Rec104p to the chromo-

somes. WD-repeat proteins have been demonstrated to act as scaffolding or adaptor proteins to interact with multiple protein partners and to carry out different roles. However, of the WD proteins characterized so far, only Ski8p shows extremely different functional roles in terms of nonoverlapping protein partners, subcellular localization, and even different target substrates (RNA vs. DNA; Arora et al. 2004).

Related to the role of Ski8p in meiosis, Ski8p has been shown to interact with Spo11p in a yeast two-hybrid system (Uetz et al. 2000; Arora et al. 2004). As discussed above, our results suggest that the interaction between Ski8p and Spo11p requires the top surface of the Ski8p structure. Moreover, the results from Arora et al. (2004) showed that alanine substitutions for residues Gln 376, Arg 377, and Glu 378 in Spo11p both abolished the Spo11p–Ski8p two-hybrid interaction and disrupted meiotic DSB formation. Based on these observations, the two surfaces of Spo11p and Ski8p required for interaction have begun to be identified. Moreover, because the F59A mutation in Ski8p also affects Spo11p interaction, it seems likely that Spo11p also interacts with the side of the  $\beta$  propeller structure to some extent.

An intriguing issue is why Ski8p is involved in both mRNA decay and meiosis. One possibility is that this bifunctional nature is simply an example of a protein being coopted for an additional use through evolution. Alternatively, the use of Ski8p in meiosis could be a way of coordinating changes in mRNA turnover with the meiotic program. This is potentially relevant because there are clear changes in mRNA decay rates during meiosis (e.g., Surosky et al. 1994). In addition, two observations raise the possibility that Ski8p function in mRNA decay might be inhibited during meiosis. First, because the Spo11p and Ski3p binding sites both require the top surface of Ski8p, the induction of Spo11p during meiosis might inhibit assembly of the Ski complex by titrating the available Ski8p. In addition, the translocation of Ski8p into the nucleus during meiosis would also be expected to limit its function in cytoplasmic mRNA decay. However, despite this intriguing connection, additional experiments will be required to test if there is a functional connection between the Ski8p role in mRNA decay and meiosis.

## Materials and methods

### *Protein expression and purification*

The full-length ORF of the budding yeast Ski8p was cloned into the pGEX-6P-1 (Amersham) and expressed as a GST-fusion protein in *E. coli*. Expression was induced by the addition of 0.1 mM isopropyl- $\beta$ -D-thio-galactoside (IPTG) when cells reached to an OD<sub>600</sub> of 0.5, and were allowed to grow for an additional 5 h at 28°C. Seleno-methionine substituted protein was expressed by growing cells in a minimal media containing 20 mg/L L-seleno-methionine (Sigma). Cells were harvested by centrifugation, re-

suspended in a lysis buffer (20 mM Tris-HCl at pH 7.6, 500 mM NaCl, 2 mM DTT, 2 mM Bendazole, 1 mM EDTA, 0.1 mM PMSF) for 30 min, and lysed by sonication. The clarified cell lysate was loaded onto a glutathione-Sepharose 4B column (Amersham). The GST-fusion protein was eluted by glutathione and cleaved by PreScission protease (Amersham) overnight at 4°C. After desalting, the cleaved protein was passed through a second glutathione-Sepharose 4B column and further purified by MonoS column (Amersham). Fractions containing Ski8 protein were combined and purified further by gel filtration chromatography on a Superdex-75 column (Amersham). Eluted fractions containing Ski8 protein were pooled and concentrated to ~6 mg/mL for crystallization.

### *Crystallization and data collection*

Crystals were grown in hanging drops at 15 °C by vapor diffusion from 28% PEG4000, 50 mM sodium citrate at pH 5.6, 20% ethylene glycol. Large crystals with typical dimensions of 0.6 × 0.2 × 0.06 mm were obtained in a period of 1–2 wk by microseeding and/or macroseeding. For data collection, crystals were harvested directly from the mother liquor and flash-cooled in liquid nitrogen, as the concentration of PEG4000 and ethylene glycol in the mother liquor is high enough for cryoprotection. The seleno-methionine derivative crystals contain one Ski8 molecule per asymmetric unit and belong to space group P2<sub>1</sub>2<sub>1</sub>2<sub>1</sub> with unit cell dimensions  $a = 66.09$  Å,  $b = 67.13$  Å,  $c = 82.01$  Å,  $\alpha = \beta = \gamma = 90^\circ$ . Multiwavelength anomalous dispersion (MAD) data for the seleno-methionine derivative were collected on a beamline BW7A at Deutsches Elektronen Synchrotron (DESY). Data were processed using DENZO (Otwinowski and Minor 1997), and intensities were reduced and scaled using SCALEPACK (Otwinowski and Minor 1997). Data statistics are summarized in Table 1.

### *Structure determination and refinement*

The structure of Ski8p was solved by MAD phasing. Four selenium sites were located using the automated Patterson search routine implemented in the program SOLVE (Terwilliger and Berendzen 1999). Phases calculated with SOLVE were further improved with the program RESOLVE (Terwilliger 2002). A partial model containing nearly 80% of the amino acids in the polypeptide chain was built automatically with RESOLVE (Terwilliger 2002). The rest of the model was built manually with the program O (Jones et al. 1991). Refinement was performed using the program CNS (Brunger et al. 1998). The final round of the refinement was carried out with the program REFMAC5 (Murshudov et al. 1997). The quality of the model was assessed with the program PROCHECK (Laskowski et al. 1993), showing that 85.7% residues lie in the most favored region with no residues in the disallowed regions in a Ramachandran plot. Crystallographic statistics are summarized in Table 1.

### *Site-directed mutagenesis and yeast two-hybrid assay*

Interaction assays between Ski8p and Ski2p, Ski3p, and Spo11p, respectively were performed by the yeast two-hybrid method using the Matchmaker3 system. Site-directed mutagenesis was performed using the Quick-Change system according to the manufacturer's instructions (Stratagene). Gal4-BD domain fusion of wild-type Ski3p, Ski2p, and Spo11p were constructed by inserting double enzyme-digested fragments into the pGBKT7 vector, using

restriction endonucleases EcoRI and BamHI, SmaI and PstI, respectively. Gal4-AD domain fusion of wild-type and mutant Ski8p were prepared by inserting restriction endonucleases NdeI and XhoI digested fragments into the pGADT7 vector. Haploid yeast strains AH109 carrying the Gal4-AD fusion protein (strains carrying only vector pGADT7 as negative control) and Y187 containing the Gal4-BD fusion protein were mated in appropriate pairwise combinations, and the resulting diploids were grown on synthetic dropout medium without leucine and tryptophan. All vectors and yeast strains used here come from Clontech. For yeast two-hybrid interactions between variant Ski8p and Ski2p/Ski3p, corresponding diploid colonies were spread on the synthetic dropout medium without tryptophan, leucine, histidine, and adenine. For  $\beta$ -galactosidase activity assay, overnight diploid cultures were diluted with fresh medium and grown to a midlog phase (3–4 h). Cells were broken by a freeze/thaw method, and the activity assay was carried out according to standard protocols (Clontech). One unit of  $\beta$ -galactosidase hydrolyzes 1  $\mu$ mole of *o*-nitrophenyl  $\beta$ -D-galactopyranoside per minute per cell.

### GST pull-down assay

Ski3p and Spo11p were translated in vitro using the recombinant plasmids pGBKT7 described above as templates in the presence of  $^{35}$ S-methionine with The TNT T7 Quick Coupled Transcription/Translation System (Promega). For GST pull-down assays, 500  $\mu$ g of GST or GST fusion Ski8p variants (wild type, Ski8-F59A, and Ski8-Topmutant) were immobilized on glutathione-Sepharose. Bound fusion proteins were incubated with 5  $\mu$ L of the in vitro translated Ski3p and Spo11p at 4°C for 1–2 h. The beads were washed five times with binding buffer (20 mM HEPES, 1 mM EDTA, 10 mM MgCl<sub>2</sub>, 4 mM DTT, 10% glycerol, 0.1 mM PMSF, 0.5% Triton X-100 at pH 7.9). Bound proteins were eluted in SDS loading buffer and resolved by SDS/PAGE (0.5  $\mu$ L of in vitro translated protein as input), and visualized by autoradiography.

### Coordinates

The coordinates and structure-factor amplitudes for Ski8p have been deposited in the Protein Data Bank with accession codes 1S4U.

### Acknowledgments

We thank Dr. Paul Tucker at BW7A (European Molecular Biology Laboratory, Hamburg, Germany) for assistance and access to synchrotron radiation facilities. This work was financially supported by the Agency for Science, Technology and Research (A\* Star) in Singapore (H.S.) and by the Howard Hughes Medical Institute (R.P.).

The publication costs of this article were defrayed in part by payment of page charges. This article must therefore be hereby marked “advertisement” in accordance with 18 USC section 1734 solely to indicate this fact.

### References

- Allmang, C., Petfalski, E., Podtelejnikov, A., Mann, M., Tollervey, D., and Mitchell, P. 1999. The yeast exosome and human PM-Scl are related complexes of 3'  $\rightarrow$  5' exonucleases. *Genes & Dev.* **13**: 2148–2158.
- Aloy, P., Botcher, B., Ceulemans, H., Leutwein, C., Mellwig, C., Fischer, S., Gavin, A.C., Bork, P., Superti-Furga, G., Serrano, L., et al. 2004. Structure-based assembly of protein complexes in yeast. *Science* **303**: 2026–2029.
- Araki, Y., Takahashi, S., Kobayashi, T., Kajihito, H., Hoshino, S., and Katada, T. 2001. Ski7p G protein interacts with the exosome and the Ski complex for 3'-to-5' mRNA decay in yeast. *EMBO J.* **20**: 4684–4693.
- Arora, C., Kee, K., Maleki, S., and Keeney, S. 2004. Antiviral protein Ski8 is a direct partner of Spo11 in meiotic DNA break formation, independent of its cytoplasmic role in RNA metabolism. *Mol. Cell* **13**: 549–559.
- Brown, J.T., Bai, X., and Johnson, A.W. 2000. The yeast antiviral proteins Ski2p, Ski3p, and Ski8p exist as a complex in vivo. *RNA* **6**: 449–457.
- Brunger, A.T., Adams, P.D., Clore, G.M., DeLano, W.L., Gros, P., Grosse-Kunstleve, R.W., Jiang, J.S., Kuszewski, J., Nilges, M., Pannu, N.S., et al. 1998. Crystallography & NMR system: A new software suite for macromolecular structure determination. *Acta Crystallogr. D* **54**: 905–921.
- Cao, D. and Parker, R. 2003. Computational modeling and experimental analysis of nonsense-mediated decay in yeast. *Cell* **113**: 533–545.
- Chen, C.Y., Gherzi, R., Ong, S.E., Chan, E.L., Rajmakers, R., Pruijn, G.J., Stoecklin, G., Moroni, C., Mann, M., and Karin, M. 2001. AU binding proteins recruit the exosome to degrade ARE-containing mRNAs. *Cell* **107**: 451–464.
- Evans, D.H., Li, Y.F., Fox, M.E., and Smith, G.R. 1997. A WD repeat protein, Rec14, essential for meiotic recombination in *Schizosaccharomyces pombe*. *Genetics* **146**: 1253–1264.
- Fox, M.E. and Smith, G.R. 1998. Control of meiotic recombination in *Schizosaccharomyces pombe*. *Prog. Nucleic Acid Res. Mol. Biol.* **61**: 345–378.
- Frischmeyer, P.A. and Dietz, H.C. 1999. Nonsense-mediated mRNA decay in health and disease. *Hum. Mol. Genet.* **8**: 1893–1900.
- Frischmeyer, P.A., van Hoof, A., O'Donnell, K., Guerrero, A.L., Parker, R., and Dietz, H.C. 2002. An mRNA surveillance mechanism that eliminates transcripts lacking termination codons. *Science* **295**: 2258–2261.
- Gardiner, J.M., Bullard, S.A., Chrome, C., and Malone, R.E. 1997. Molecular and genetic analysis of REC103, an early meiotic recombination gene in yeast. *Genetics* **146**: 1265–1274.
- Gaudet, R., Bohm, A., and Sigler, P.B. 1996. Crystal structure at 2.4 angstroms resolution of the complex of transducin  $\beta$  and its regulator, phosducin. *Cell* **87**: 577–588.
- Goebl, M. and Yanagida, M. 1991. The TPR snap helix: A novel protein repeat motif from mitosis to transcription. *Trends Biochem. Sci.* **16**: 173–177.
- Jacobs Anderson, J.S. and Parker, R. 1998. The 3' to 5' degradation of yeast mRNAs is a general mechanism for mRNA turnover that requires the SKI2 DEVH box protein and 3' to 5' exonucleases of the exosome complex. *EMBO J.* **17**: 1497–1506.
- Jones, T.A., Zou, J.Y., Cowan, S.W., and Kjeldgaard, M. 1991. Improved methods for building protein models in electron density maps and the location of errors in these models. *Acta Crystallogr. A* **47**: 110–119.
- Komachi, K. and Johnson, A.D. 1997. Residues in the WD repeats of Tup1 required for interaction with  $\alpha$ 2. *Mol. Cell Biol.* **17**: 6023–6028.
- Kraulis, P.J. 1991. MOLSCRIPT: A program to produce both detailed and schematic plots of protein structures. *J. Appl. Crystallogr.* **24**: 946–950.
- Lambright, D.G., Sondek, J., Bohm, A., Skiba, N.P., Hamm, H.E., and Sigler, P.B. 1996. The 2.0 Å crystal structure of a heterotrimeric G protein. *Nature* **379**: 311–319.
- Laskowski, R.A., Moss, D.S., and Thornton, J.M. 1993. Main-chain bond lengths and bond angles in protein structures. *J. Mol. Biol.* **231**: 1049–1067.
- Lejeune, F., Li, X., and Maquat, L.E. 2003. Nonsense-mediated mRNA decay in mammalian cells involves decapping, deadenylation, and exonucleolytic activities. *Mol. Cell* **12**: 675–687.
- Malone, R.E., Bullard, S., Hermiston, M., Rieger, R., Cool, M., and Galbraith, A. 1991. Isolation of mutants defective in early steps of meiotic recombination in the yeast *Saccharomyces cerevisiae*. *Genetics* **128**: 79–88.
- Maquat, L.E. 2002. Molecular biology. Skiing toward nonstop mRNA decay. *Science* **295**: 2221–2222.
- Masison, D.C., Blanc, A., Ribas, J.C., Carroll, K., Sonenberg, N., and Wickner, R.B. 1995. Decoying the cap-mRNA degradation system by a double-stranded RNA virus and poly(A)-mRNA surveillance by a yeast antiviral system. *Mol. Cell Biol.* **15**: 2763–2771.
- Matsumoto, Y., Sarkar, G., Sommer, S.S., and Wickner, R.B. 1993. A yeast antiviral protein, SKI8, shares a repeated amino acid sequence pattern with  $\beta$ -subunits of G proteins and several other proteins. *Yeast* **9**: 43–51.
- Mitchell, P. and Tollervey, D. 2001. mRNA turnover. *Curr. Opin. Cell Biol.* **13**: 320–325.
- . 2003. An NMD pathway in yeast involving accelerated deadenylation and exosome-mediated 3'  $\rightarrow$  5' degradation. *Mol. Cell* **11**: 1405–1413.
- Mitchell, P., Petfalski, E., Shevchenko, A., Mann, M., and Tollervey, D. 1997. The exosome: A conserved eukaryotic RNA processing complex containing multiple 3'  $\rightarrow$  5' exoribonucleases. *Cell* **91**: 457–466.
- Muhlrad, D. and Parker, R. 1994. Premature translational termination triggers mRNA decapping. *Nature* **370**: 578–581.

- Mukherjee, D., Gao, M., O'Connor, J.P., Raijmakers, R., Pruijn, G., Lutz, C.S., and Wilusz, J. 2002. The mammalian exosome mediates the efficient degradation of mRNAs that contain AU-rich elements. *EMBO J.* **21**: 165–174.
- Murshudov, G.N., Vagin, A.A., and Dodson, E.J. 1997. Refinement of macromolecular structures by the maximum-likelihood method. *Acta Crystallogr. D* **53**: 240–255.
- Neer, E.J., Schmidt, C.J., Nambudripad, R., and Smith, T.F. 1994. The ancient regulatory-protein family of WD-repeat proteins. *Nature* **371**: 297–300.
- Nicholls, A., Sharp, K.A., and Honig, B. 1991. Protein folding and association: Insights from the interfacial and thermodynamic properties of hydrocarbons. *Proteins* **11**: 281–296.
- Otwinowski, Z. and Minor, W. 1997. Processing of X-ray diffraction data collected in oscillation mode. *Methods Enzymol.* **276**: 307–326.
- Parker, R. and Song, H. 2004. The enzymes and control of eukaryotic mRNA turnover. *Nat. Struct. Mol. Biol.* **11**: 121–127.
- Pecina, A., Smith, K.N., Mezard, C., Murakami, H., Ohta, K., and Nicolas, A. 2002. Targeted stimulation of meiotic recombination. *Cell* **111**: 173–184.
- Pickles, L.M., Roe, S.M., Hemingway, E.J., Stifani, S., and Pearl, L.H. 2002. Crystal structure of the C-terminal WD40 repeat domain of the human Groucho/TLE1 transcriptional corepressor. *Structure (Camb)* **10**: 751–761.
- Rhee, S.K., Icho, T., and Wickner, R.B. 1989. Structure and nuclear localization signal of the SKI3 antiviral protein of *Saccharomyces cerevisiae*. *Yeast* **5**: 149–158.
- Smith, T.F., Gaitatzes, C., Saxena, K., and Neer, E.J. 1999. The WD repeat: A common architecture for diverse functions. *Trends Biochem. Sci.* **24**: 181–185.
- Sondek, J., Bohm, A., Lambright, D.G., Hamm, H.E., and Sigler, P.B. 1996. Crystal structure of a G-protein  $\beta$   $\gamma$  dimer at 2.1 Å resolution. *Nature* **379**: 369–374.
- Sprague, E.R., Redd, M.J., Johnson, A.D., and Wolberger, C. 2000. Structure of the C-terminal domain of Tup1, a corepressor of transcription in yeast. *EMBO J.* **19**: 3016–3027.
- Surosky, R.T., Strich, R., and Esposito, R.E. 1994. The yeast UME5 gene regulates the stability of meiotic mRNAs in response to glucose. *Mol. Cell Biol.* **14**: 3446–3458.
- Takahashi, S., Araki, Y., Sakuno, T., and Katada, T. 2003. Interaction between Ski7p and Upf1p is required for nonsense-mediated 3'-to-5' mRNA decay in yeast. *EMBO J.* **22**: 3951–3959.
- Terwilliger, T.C. 2002. Automated structure solution, density modification and model building. *Acta Crystallogr. D* **58**: 1937–1940.
- Terwilliger, T.C. and Berendzen, J. 1999. Automated MAD and MIR structure solution. *Acta Crystallogr. D* **55**: 849–861.
- Tesse, S., Storlazzi, A., Kleckner, N., Gargano, S., and Zickler, D. 2003. Localization and roles of Ski8p protein in *Sordaria meiosis* and delineation of three mechanistically distinct steps of meiotic homolog juxtaposition. *Proc. Natl. Acad. Sci.* **100**: 12865–12870.
- Toh, E., Guerry, P., and Wickner, R.B. 1978. Chromosomal superkiller mutants of *Saccharomyces cerevisiae*. *J. Bacteriol.* **136**: 1002–1007.
- Tucker, M. and Parker, R. 2000. Mechanisms and control of mRNA decapping in *Saccharomyces cerevisiae*. *Annu. Rev. Biochem.* **69**: 571–595.
- Uetz, P., Giot, L., Cagney, G., Mansfield, T.A., Judson, R.S., Knight, J.R., Lockshon, D., Narayan, V., Srinivasan, M., Pochart, P., et al. 2000. A comprehensive analysis of protein-protein interactions in *Saccharomyces cerevisiae*. *Nature* **403**: 623–627.
- van der Voorn, L. and Ploegh, H.L. 1992. The WD-40 repeat. *FEBS Lett.* **307**: 131–134.
- van Hoof, A. and Parker, R. 1999. The exosome: A proteasome for RNA? *Cell* **99**: 347–350.
- van Hoof, A., Lennertz, P., and Parker, R. 2000. Yeast exosome mutants accumulate 3'-extended polyadenylated forms of U4 small nuclear RNA and small nucleolar RNAs. *Mol. Cell Biol.* **20**: 441–452.
- van Hoof, A., Frischmeyer, P.A., Dietz, H.C., and Parker, R. 2002. Exosome-mediated recognition and degradation of mRNAs lacking a termination codon. *Science* **295**: 2262–2264.
- Voegtli, W.C., Madrona, A.Y., and Wilson, D.K. 2003. The structure of Aip1p, a WD repeat protein that regulates Cofilin-mediated actin depolymerization. *J. Biol. Chem.* **278**: 34373–34379.
- Wall, M.A., Coleman, D.E., Lee, E., Iniguez-Lluhi, J.A., Posner, B.A., Gilman, A.G., and Sprang, S.R. 1995. The structure of the G protein heterotrimer  $G_i \alpha 1 \beta 1 \gamma 2$ . *Cell* **83**: 1047–1058.
- Wang, Z. and Kiledjian, M. 2001. Functional link between the mammalian exosome and mRNA decapping. *Cell* **107**: 751–762.
- Waterhouse, P.M., Wang, M.B., and Lough, T. 2001. Gene silencing as an adaptive defence against viruses. *Nature* **411**: 834–842.
- Widner, W.R. and Wickner, R.B. 1993. Evidence that the SKI antiviral system of *Saccharomyces cerevisiae* acts by blocking expression of viral mRNA. *Mol. Cell Biol.* **13**: 4331–4341.
- Wu, G., Xu, G., Schulman, B.A., Jeffrey, P.D., Harper, J.W., and Pavletich, N.P. 2003. Structure of a  $\beta$ -TrCP1-Skp1- $\beta$ -catenin complex: Destruction motif binding and lysine specificity of the SCF( $\beta$ -TrCP1) ubiquitin ligase. *Mol. Cell* **11**: 1445–1456.